

Chemical kinetic and radiating species studies of Titan aerocapture entry

Pénélope Leyland¹, Raffaello Sobbia², and Jan B. Vos³

¹ STI-ISE-LIN, Station 9, Ecole Polytechnique Fédérale de Lausanne, CH-1015 Lausanne, Switzerland

² CRPP - Centre of Research on Plasma Physics, Ecole Polytechnique Fédérale de Lausanne, CH-1015 Lausanne, Switzerland

³ CFS Engineering, CH-1015 Lausanne, Switzerland

Abstract

TITAN Aerocapture entry has been studied in collaboration with the Hypersonics Centre of the University Queensland (UQ), Australia. The simulation of the experimental conditions and also the flight conditions are made using CFD coupled with chemistry libraries of which CHEMKIN. This can be compared to in-code implementation for the Earth reentry. Reduced models based on combustion data bases are taken for the reactions data set for Titan's entry.

Introduction

To improve our knowledge of (re-)entry phenomenon around space vehicles it is necessary to understand the chemical kinetic mechanisms present in the flowfield between the strong bow shock and the vehicle surface. Indeed the strong shock triggers off chemical reactions of the species of the atmosphere, with dissociation, recombination and creation of derived species. In particular the hot gas can become radiating, dependent on the composition. The use of Computational Fluid Dynamics (CFD) as a tool to simulate the external aerothermodynamics over vehicles, requires significant physical modelisation in order to correctly represent the phenomena taking place within entry. Backed up by analytical techniques for margin estimations and scaling parameters, experimental means are necessary in order to achieve ground measurements that either cannot or were not part of the on-board flight experimentation. To improve the modelisation, a large amount of effort should be put into the development of a chemical model adapted to the chemistry of the entry phase. For Earth reentry, several well developed models exist for hypersonics, such as Park's model and its extensions, [1]. The radiating component is difficult to achieve in ground facilities due to binary scaling, [3]. For other planetary atmospheres, the gaseous composition of the atmosphere can be challenging. One of these is given by the Titan's aerocapture flight where the outer atmosphere is composed of methane, nitrogen (approximately 5 and 88 % respectively) and argon (0 to 10 %). Here the chemical reactions are close to hydrocarbone ones, with many derived species, in particular the highly radiating CN, and ionisation products. The kinetic model is hence complex, and includes a high number of species. Work of Park, Nelson and co-authors have derived models, that are resumed and analysed by T. Gökçen, who has presented a specific reduced model, [4]. The interest of the Titan aerocapture conditions is that radiation is not annulled by binary scaling and remains present in the ground facilities.

To simulate with CFD the complete aerothermodynamic flowfield over the Titan entry capsule means that a high number of species equations must be added to the reactive Navier Stokes equations. This results in a very large system. For convergence requirements, the use of implicit techniques lead to severe memory problems even on the largest systems available. This is even true for the reduced model proposed by T. Gökçen. Also, the coupling of the chemical kinetic modeling and the flow solver is highly complex. For this reason the use of coupling the Navier-

Stokes real gas solver with a chemical kinetic mechanism library of CHEMKIN has been adopted here. In order to have a chance to compute, a further reduced model has been devised which takes into account the main features. This mechanism is tested over equivalent cylinders to the flight and experimental models. Particular attention is made on the relative importance of ionised species and electrons.

Validation of the Reduced Chemical Model

The Titan atmosphere gas is simplified by taking an initial composition of 95% N₂ and 5% CH₄, as in the UQ experiments. To obtain a reduced model the following analysis was made: first a sensitivity analysis of rate-limiting steps in production/consumption species using CHEMKIN, second, the CFD results on small cylinder geometry in the conditions of flight and the ground experiments in X3 were analysed to see which species were negligible. It was seen that the argon components can be ignored, as well as the ionisation species of C⁺, CH⁺, H⁺ and N₂⁺.

Validation of the present model has been made against the reduced Gökçen model [4] using the SENKIN and SHOCK programs in the CHEMKIN package [5] for a shock tube without boundary layer correction with incident shock velocity of 6.3 km/s, pressure of 0.1 Torr, and temperature before the shock of 300 K. The reaction set is presented in table 2, which consists of 13 neutral chemical species (C₂, C, CH₄, CH₃, CH₂, CH, CN, H₂, H, N₂, N, HCN, NH), two positive ions (CN⁺, N⁺), and electrons (E). The fits to C_p^0/R , H^0/RT and S^0/R consist of seven coefficients for the temperature range from 300 to 20000 K. The downstream model equations assume that the flow is adiabatic and that the transport phenomena associated with mass diffusion thermal conduction and viscous effects are negligible [5]. Figure 1 and figure 2 show the variation of representative species mole fractions with respect to time.

A very good agreement between the present reduced model and the Gökçen's reduced model is achieved for the computed neutral species considered in this work, 1. However, this is not the case for the ionised species. CN⁺ shows a longer relaxation time and relaxes to a higher value in the present reduced model than in Gökçen's one. For N⁺, both models show the same trend, but Gökçen's model gives higher values. For electrons, the behaviour is quite different. Gökçen's model give a strong rise, whereas our model first shows a local maximum and then decreases towards a lower value.

CFD Results with the Chemical Model

The model is tested by considering the flow over a cylinder in the same flight and ground facilities of the X3 expansion tube at UQ. The flow conditions are as follows, see table 1.

The results over the cylinder show complete and immediate dissociation of CH₄ behind the shock in both flight and X3 flow fields, with creation of highly radiating CN in the shock layer,

| | Flight | X3 -UQ 1:40.7 Model |
|-------------------------------|-----------------------|-----------------------|
| $V_{km/s}$ | 5.76 | 5.83 |
| ρ (kg/m ³) | 1.49×10^{-4} | 2.43×10^{-3} |
| ρL (kg/m ²) | 5.2×10^{-4} | 5.2×10^{-4} |
| p Pa | 6.9 | 1130 |
| α AOA | 16° | 16° |

Table 1: Flowfield conditions - Flight and X3 for Titan aerocapture entry

see figure 3. A significant quantity of N⁺ is also produced, see figure 4. The difference with Gökçen's reduced model is a loss of species away from the stagnation centreline, (seen by diffusion near the corners). The electronic component is evident near the surface in flight conditions, and also is present in X3 conditions, figure 4. This plasma "creation" could be of significant importance also for measurement techniques. Coupled calculations on the Titan capsule were made for X3 conditions and compared to measurements of B. Capra [3]. The flow field is shown in figure 5. The comparison of the heatfluxes between the CFD and the X3 results were reasonable: $0.78kW/cm^2$ for the heat flux in the stagnation region for the CFD against $0.7kW/cm^2$ for the X3 experiment, and $0.6kW/cm^2$ at an exterior point for the CFD, against $0.5kW/cm^2$ at the same position for the experiments.

References

- [1] Park, C. "Non equilibrium hypersonic aerothermodynamics". John Wiley and Sons. 1990
- [2] Capra, B. R., Morgan, R. G., and Leyland, P., in *Aerothermodynamics for Space Vehicles, Cologne, ESA Publications 2005*.
- [3] B. Capra. Ph D Thesis. University Queensland, AUS. 2006.
- [4] Gökçen, T., "N₂-CH₄-Ar chemical kinetic model for simulations of atmospheric entry to Titan", *AIAA*, 2004-2469.
- [5] The CHEMKIN collection, Release 4.1, Reaction Design, Inc., San Diego, CA, USA.

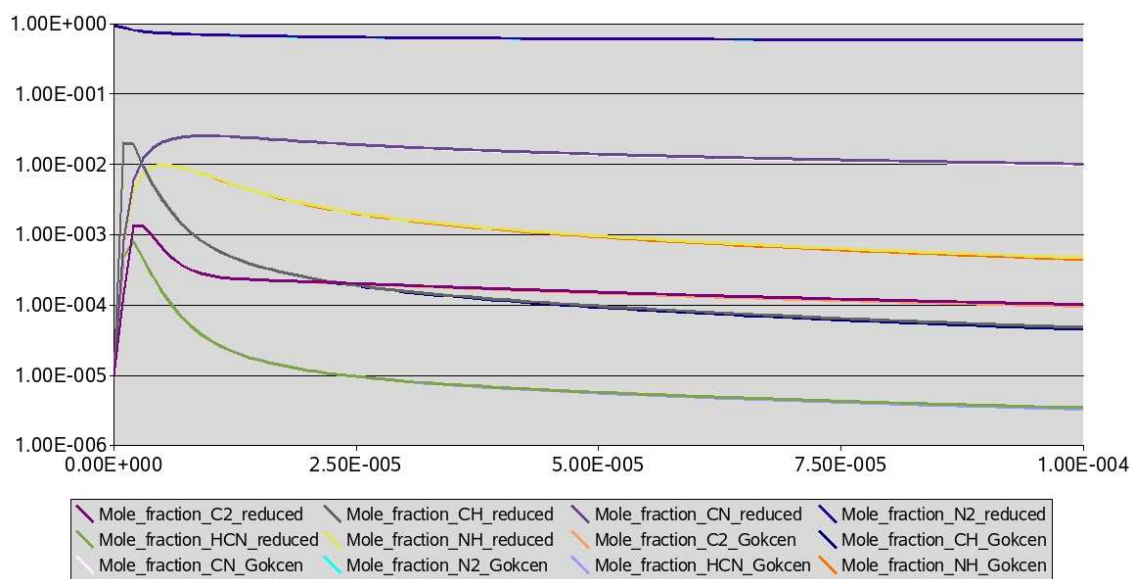


Figure 1: Time histories of computed neutral mole fractions using the reduced model of Gökçen, labeled as Gokcen, and the present reduced model, labeled as reduced.

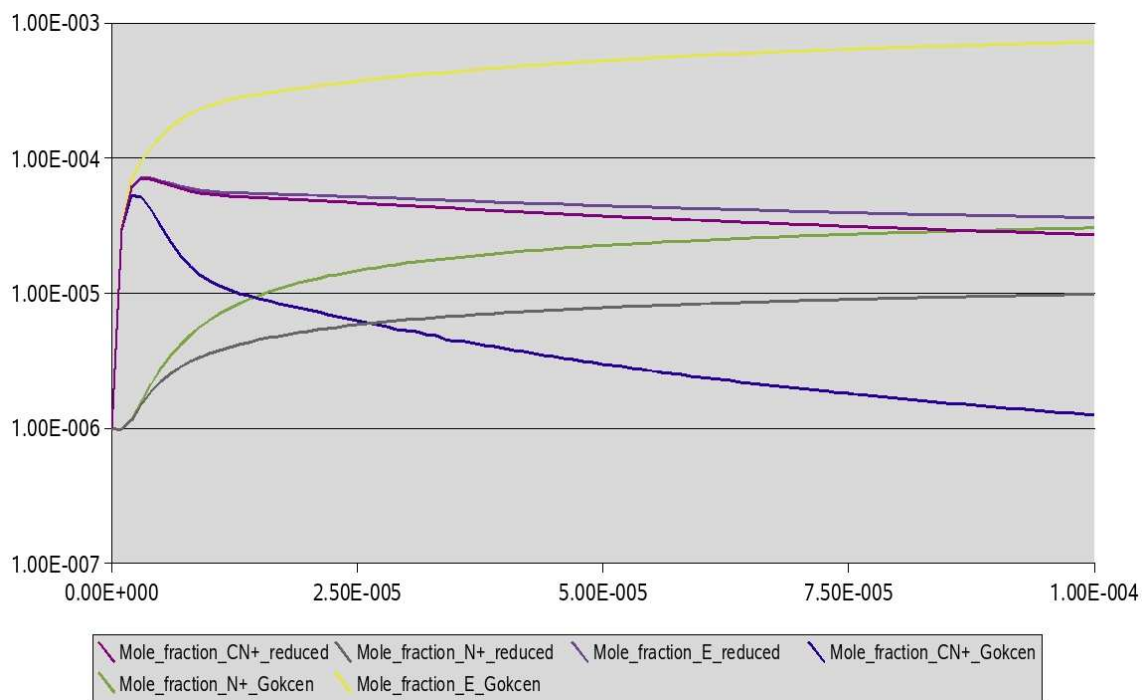


Figure 2: Time histories of computed charged particle mole fractions using the reduced model of Gökçen, labeled as Gokcen, and the present reduced model, labeled as reduced.

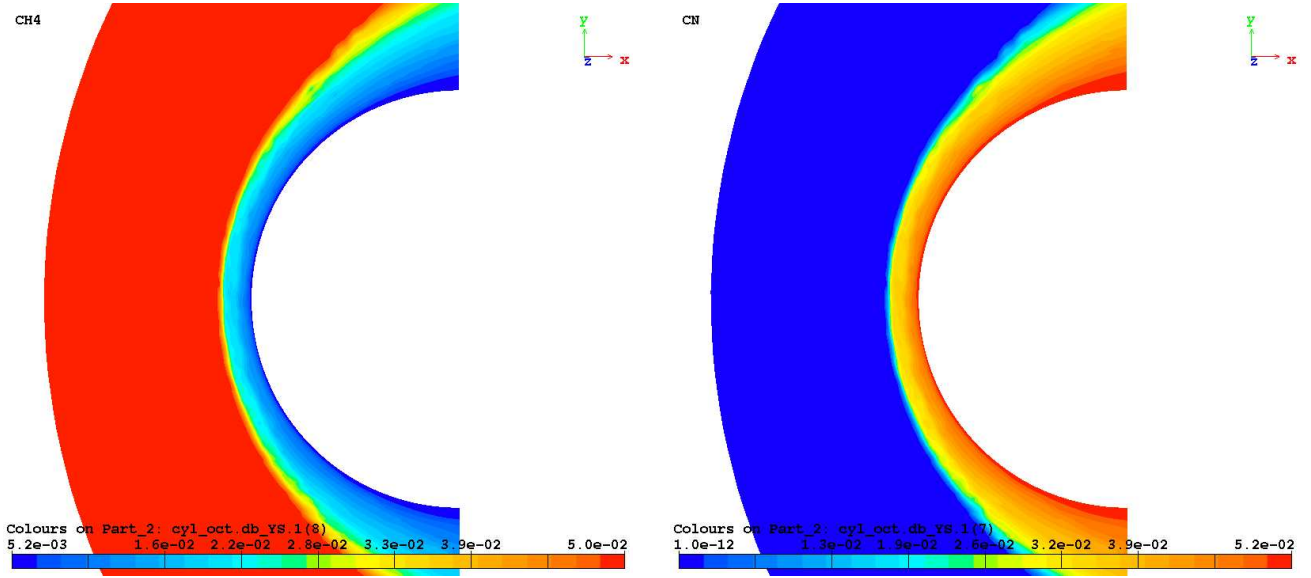


Figure 3: CH4 dissociation (left) and one of the products, CN, (right) in Titan Flight flowfield conditions

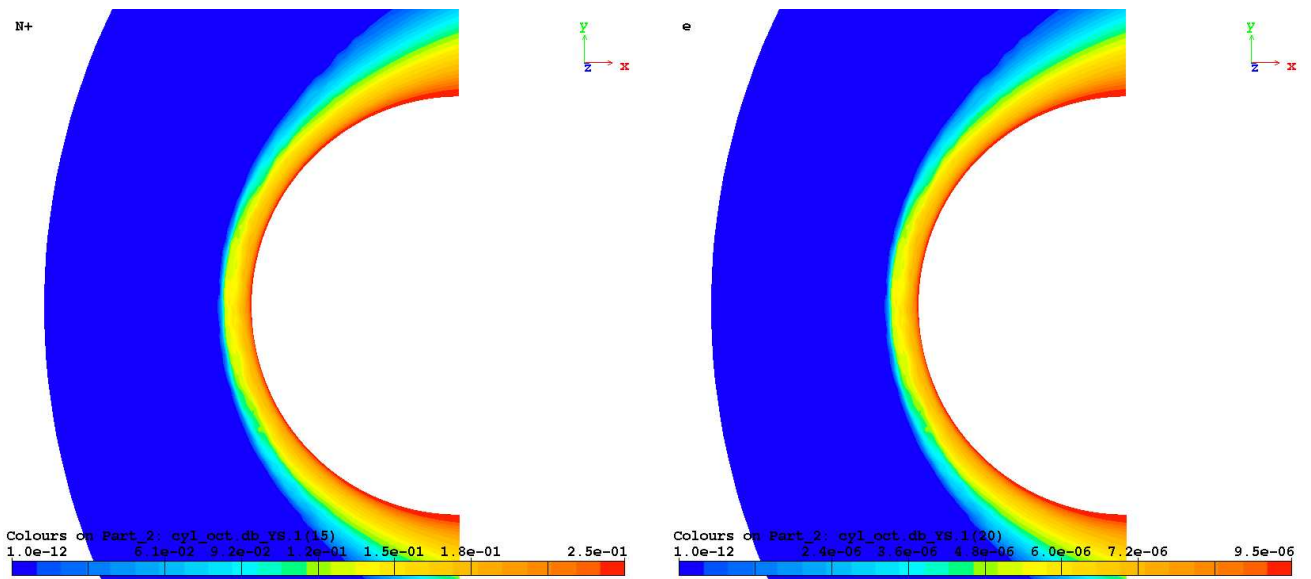


Figure 4: N+ population in the shock layer (left), max. 0.25; electron population (right), max. 10^{-5}

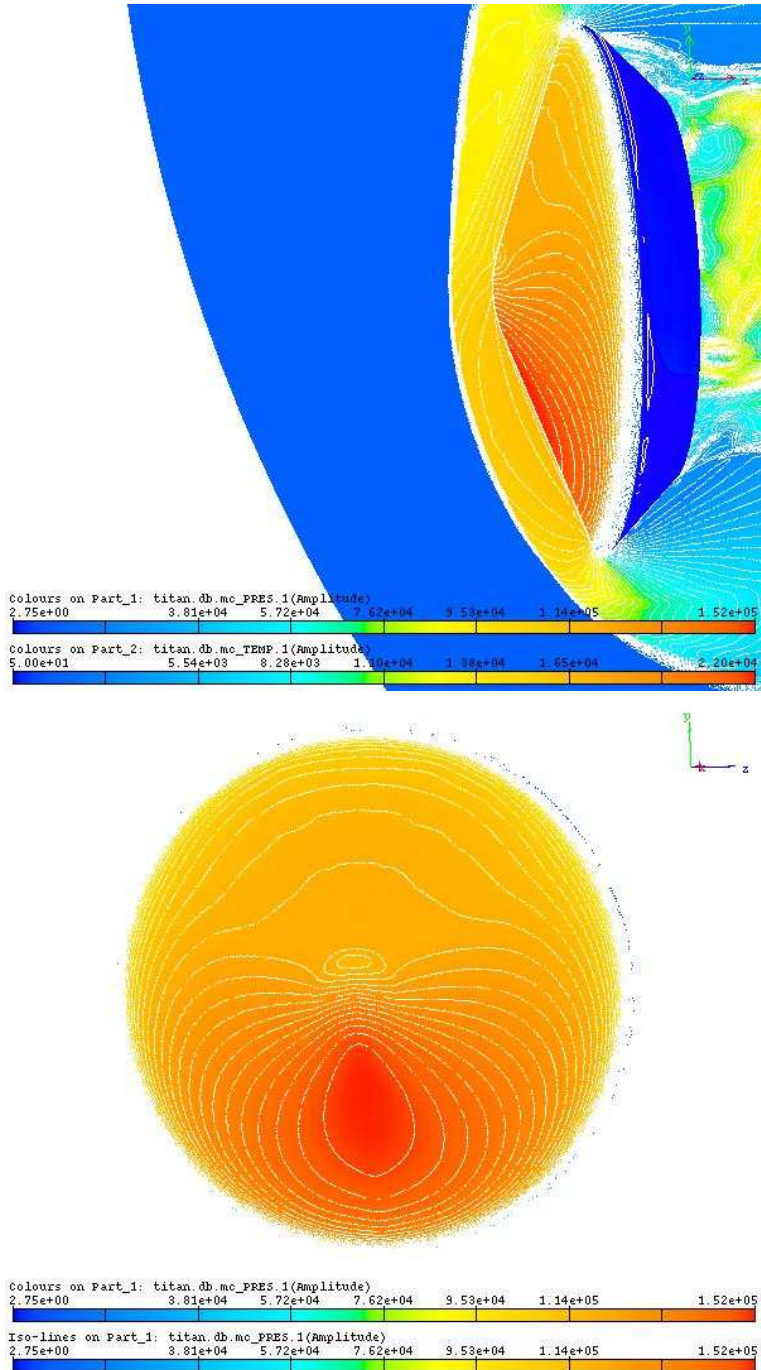


Figure 5: Titan flowfield in X3 conditions: temperature contours shows the shock structure (top), and the pressure field on the capsule surface (bottom).

| Reaction & Forward reaction rate coefficients $T_a = (T T_v)^{0.5}$ | | | |
|---|-----------------------|-------|----------|
| $k_f = AT^n e^{-\frac{E_a}{T}}$ [$cm^3/mole-s$] | $A(cc/mol/s)$ | n | $T_a(K)$ |
| Dissociation Reactions of N2 | | | |
| $N_2 + N_2 \rightarrow N + N + N_2$ | 7.00×10^{21} | -1.6 | -113200 |
| $N_2 + CH_4 \rightarrow N + N + CH_4$ | 7.00×10^{21} | -1.6 | -113200 |
| $N_2 + CH_3 \rightarrow N + N + CH_3$ | 7.00×10^{21} | -1.6 | -113200 |
| $N_2 + CH_2 \rightarrow N + N + CH_2$ | 7.00×10^{21} | -1.6 | -113200 |
| $N_2 + CH \rightarrow N + N + CH$ | 7.00×10^{21} | -1.6 | -113200 |
| $N_2 + C_2 \rightarrow N + N + C_2$ | 7.00×10^{21} | -1.6 | -113200 |
| $N_2 + H_2 \rightarrow N + N + H_2$ | 7.00×10^{21} | -1.6 | -113200 |
| $N_2 + CN \rightarrow N + N + CN$ | 7.00×10^{21} | -1.6 | -113200 |
| $N_2 + NH \rightarrow N + N + NH$ | 7.00×10^{21} | -1.6 | -113200 |
| $N_2 + HCN \rightarrow N + N + HCN$ | 7.00×10^{21} | -1.6 | -113200 |
| $N_2 + N \rightarrow N + N + N$ | 3.0×10^{22} | -1.6 | -113200 |
| $N_2 + C \rightarrow N + N + C$ | 3.0×10^{22} | -1.6 | -113200 |
| $N_2 + H \rightarrow N + N + H$ | 3.0×10^{22} | -1.6 | -113200 |
| $N_2 + CN^+ \rightarrow N + N + CN^+$ | 7.00×10^{21} | -1.6 | -113200 |
| $N_2 + N^+ \rightarrow N + N + N^+$ | 7.00×10^{21} | -1.6 | -113200 |
| $N_2 + E \rightarrow N + N + E$ | 3.0×10^{24} | -1.6 | -1132000 |
| Dissociation Reactions of CH4, CH3, CH2, CH | | | |
| $CH_4 + M \rightarrow CH_3 + H + M$ | 4.70×10^{47} | -8.2 | -59200 |
| $CH_3 + M \rightarrow CH_2 + H + M$ | 1.02×10^{16} | 0 | -45600 |
| $CH_3 + M \rightarrow CH + H_2 + M$ | 5.00×10^{15} | 0 | -42800 |
| $CH_2 + M \rightarrow CH + H + M$ | 9.68×10^{15} | 0 | -41800 |
| $CH_2 + M \rightarrow C + H_2 + M$ | 9.68×10^{14} | 0 | -29700 |
| $CH + M \rightarrow C + H + M$ | 9.68×10^{14} | 0 | -33700 |
| Dissociation Reactions of C2 | | | |
| $C_2 + M \rightarrow C + C + M$ | 1.50×10^{16} | 0 | -71600 |
| Dissociation Reactions of H2 | | | |
| $H_2 + M \rightarrow H + H + M$ | 2.23×10^{14} | 0 | -48350 |
| Dissociation Reactions of CN | | | |
| $CN + M \rightarrow C + N + M$ | 2.53×10^{14} | 0 | -71000 |
| Dissociation Reactions of NH | | | |
| $NH + M \rightarrow N + H + M$ | 1.8×10^{14} | 0 | -37600 |
| Dissociation Reactions of HCN | | | |
| $HCN + M \rightarrow CN + H + M$ | 3.57×10^{26} | -2.6 | -62845 |
| CH3 Radical Reactions | | | |
| $CH_3 + N \rightarrow HCN + H + H$ | 7.0×10^{13} | 0 | 0.0 |
| $CH_3 + H \rightarrow CH_2 + H_2$ | 6.03×10^{13} | 0 | -7600 |
| CH2 Radical Reactions | | | |
| $CH_2 + N_2 \rightarrow HCN + NH$ | 4.82×10^{12} | 0 | -18000 |
| $CH_2 + N \rightarrow HCN + H$ | 5.00×10^{13} | 0 | 0.0 |
| $CH_2 + H \rightarrow CH + H_2$ | 6.03×10^{12} | 0 | +900 |
| CH Radical Reactions | | | |
| $CH + N_2 \rightarrow HCN + N$ | 4.40×10^{12} | 0 | -11060 |
| $CH + C \rightarrow C_2 + H$ | 2.00×10^{14} | 0 | 0.0 |
| C2 Radical Reactions | | | |
| $C_2 + N_2 \rightarrow CN + CN$ | 1.50×10^{13} | 0 | -21000 |
| CN Radical Reactions | | | |
| $CN + H_2 \rightarrow HCN + H$ | 2.95×10^{05} | 0 | -1130 |
| $CN + C \rightarrow C_2 + N$ | 5.00×10^{13} | 0 | -13000 |
| N-Atom Radical Reactions | | | |
| $N + H_2 \rightarrow NH + H$ | 1.60×10^{14} | 0 | -12650 |
| C-Atom Radical Reactions | | | |
| $C + N_2 \rightarrow CN + N$ | 5.24×10^{13} | 0 | -22600 |
| $C + H_2 \rightarrow CH + H$ | 9.68×10^{22} | 0 | -11700 |
| H-Atom Radical Reactions | | | |
| $H + N_2 \rightarrow NH + N$ | 3.00×10^{12} | 0.5 | -71400 |
| $H + CH_4 \rightarrow CH_3 + H_2$ | 1.32×10^{04} | 3 | -4045 |
| Associative Ionization Reactions | | | |
| $C + N \rightarrow CN^+ + E$ | 1.00×10^{15} | 1.5 | -164400 |
| Ionization Reactions (Electron-impact) | | | |
| $N + E \rightarrow N^+ + E + E$ | 2.50×10^{34} | -3.82 | -168600 |
| Charge Exchange Reactions | | | |
| $CN^+ + N \rightarrow CN + N^+$ | 9.8×10^{12} | 0 | -40700 |